Available online at www.sciencedirect.com
ScienceDirect
International Journal of Solids and Structures 44 (2007) 3887–3903
INTERNATIONAL JOURNAL OF SOLIDS and STRUCTURES
www.elsevier.com/locate/ijsolstr

Closed-form solution for the contact problem of reinforced pin-loaded joints used in glass structures

Q.D. To [a,b], Q.-C. He [b,*], M. Cossavella [a], K. Morcant [a], A. Panait [a]

[a] *Centre Scientifique et Technique du Bâtiment (CSTB), 84 Avenue Jean Jaurès, 77447 Marne-la-Vallée Cedex 2, France*
[b] *Laboratoire de Mécanique (LaM), Université de Marne-la-Vallée, 5 Boulevard Descartes, 77454 Marne-la-Vallée Cedex 2, France*

Received 2 May 2006; received in revised form 13 October 2006
Available online 3 November 2006

Abstract

In a typical pin-loaded joint used to assemble glass plates, the hole in a glass plate is reinforced by a steel ring glued to the glass plate via a soft resin layer. Thus, the ring is in direct contact with the steel bolt and prevents the glass plate from high stress concentration. This paper proposes an analytical approach to solving the resulting conforming contact problem. The strain and stress fields inside the resin layer are first determined by exploiting the fact that the stiffness of the material constituting it is much smaller than the stiffness of steel and glass. After finding the relevant Green functions for the ring and pin, the frictionless contact between them is then formulated in terms of an integral equation with a Fourier series as the kernel. This integral equation is solved by neglecting the terms of high orders and transforming it into the Cauchy singular integral equation. The derived analytical results for the contact pressure and angle are finally compared to and validated by those obtained by the finite element method.

Keywords: Contact; Pin-loaded joints; Stress analysis; Glass; Singular integral equation

1. Introduction

Glass is now used as a structural building material in the construction of facades and roofs, owing not only to its light transparency and aestheticism but also to the durability of its physico-chemical properties. Pin-loaded joints are one of the techniques used to assemble glass beams or plates. In a pin-loaded joint, stress concentration appears usually near the hole of a finite-dimension glass plate and considerably reduces the strength of the latter. For this reason, a holed glass plate is in practice reinforced along its hole border by a steel ring glued to the plate with the help of a soft resin layer, so that the ring is in direct contact with the steel bolt and protects the glass plate from high stress concentration (Fig. 1). The work presented in this paper aims to give an analytical approximate solution for this contact problem and to check the degree of precision of the solution by comparing it with the results obtained from the finite element method.

* Corresponding author. Tel.: +33 160 957 786; fax: +33 160 957 799.
E-mail address: he@univ-mlv.fr (Q.-C. He).

0020-7683/$ - see front matter
doi:10.1016/j.ijsolstr.2006.10.030

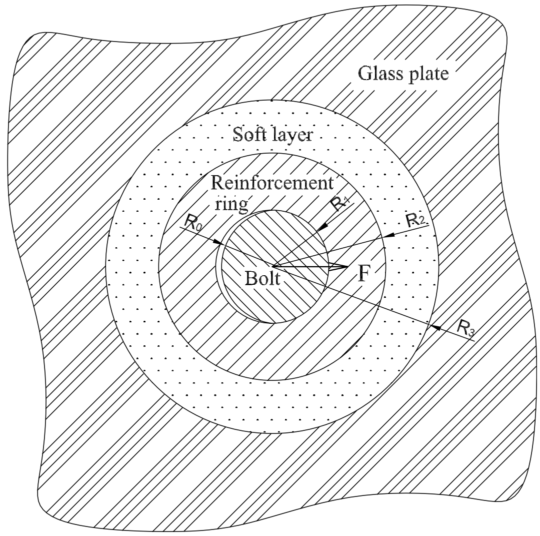

Fig. 1. Composition of a typical pin-loaded joint in a glass structure.

The layer between the steel ring and the glass plate consists of a resin which is very soft compared with steel or glass. Indeed, its typical Young modulus is about 2 GPa, while those of steel and glass are about 200 and 70 GPa, respectively. Consequently, the strain and stress fields in the layer are essentially due to the relative displacements of the steel ring and glass plate which can be both taken to be practically rigid. Thus, once the strain and stress fields in the layer are determined, the conforming contact between the bolt and the ring, assumed to be frictionless, corresponds to that of a pin with a holed finite two-dimension body undergoing stresses on its external boundary. In the literature dealing with the contact problem of pin-loaded joints as in Noble and Hussain (1969), Hyer and Klang (1985), Ciavarella and Decuzzi (2001), Lin and Lin (1999), Iyer (2001), analytical approximate solutions are limited to the case of infinite holed plates and numerical solutions are provided for the case of finite holed plates. A comprehensive review on elastic analysis of pin-loaded joints was given by Rao (1978) (see also the recent paper of Ciavarella et al. (2006) and the references cited therein). In the present work, both analytical and numerical solutions are given and compared in the case of a finite holed plate.

The paper is structured as follows. In Section 2, the unilateral frictionless contact conditions are first specified for a pin-loaded joint. The stress and displacement fields in the intermediate layer between the pin and ring are then determined. The establishment of the general integral equation governing the contact pressure and angle is carried out by finding the relevant Green functions for the pin and ring. In Section 3 where the second Dundurs parameter is assumed to be equal to zero, the analytical approximate solutions for the contact pressure and angle are derived and compared with the results obtained by the finite element method. In Section 4, a few closing remarks are drawn.

In this work, each component of a pin-loaded joint is taken to be made of a linearly elastic isotropic material. The results presented in this paper are valid both for the case of plane stress and the case of plane strain provided use is made of the corresponding Kosolov constants κ_i and μ_i which are related to the Young's modulus E_i and Poisson's ratio v_i by

$$\mu_i = \frac{E_i}{2(1+v_i)}, \quad \kappa_i = \frac{3-v_i}{1+v_i} \quad \text{(plane stress)}, \quad \kappa_i = 3-4v_i \quad \text{(plane strain)}.$$

In practice, we adopt the plane stress or strain assumption according as the thickness of the components of the pin-loaded joint is sufficiently small or large with respect to their in-plane dimensions. In what follows, the subscripts 0, 1, 2, and 3 refer, respectively, to the bolt, ring, resin layer, and glass plate of a pin-loaded joint (Fig. 1).

2. Establishment of the governing integral equation

2.1. Unilateral contact conditions

Consider a bolt of radius R_0 submitted to a horizontal concentrated force F at its center. It comes into contact with the border of a hole of radius R_1 as in Fig. 2. In what follows, contact is assumed to be frictionless and displacements are taken to be small. At the initial instant $t = 0$, the centers of the hole and bolt are located at the origin of a polar coordinate system.

The initial gap between a generic point $X_0 = (R_0, \theta)$ of the bolt border and its radial projection $X_1 = (R_1, \theta)$ on the hole border is

$$\|X_1 - X_0\| = R_1 - R_0 = \Delta R. \tag{1}$$

At the instant $t > 0$ when the contact takes place, the initial normal gap between X_0 and X_1 is closed. So, the radial displacement $u_{r0}(\theta)$ of X_0, the radial displacement $u_{r1}(\theta)$ of X_1, and the corresponding contact pressure $p(\theta)$ verify the following unilateral contact conditions:

$$\begin{aligned} &u_{r0}(\theta) - u_{r1}(\theta) = \Delta R, \quad p(\theta) \geqslant 0 \quad \theta \in [-\alpha, \alpha], \\ &u_{r0}(\theta) - u_{r1}(\theta) < \Delta R, \quad p(\theta) = 0 \quad \theta \notin [-\alpha, \alpha]. \end{aligned} \tag{2}$$

Above, the angular interval $[-\alpha, \alpha]$ defines the contact zone which is unknown at this stage, and a compressive normal stress (e.g., a pressure) is considered as positive. The main purpose of this section is to specify the displacement contact condition $u_{r0}(\theta) - u_{r1}(\theta) = \Delta R$ in terms of an integral equation.

2.2. Determination of the stress field in the intermediate layer

To derive $u_{r1}(\theta)$ in (2), we consider a fundamental problem where the ring is subject to a horizontal unitary force P on the border as in Fig. 3. The intermediate layer between the steel ring and the glass plate is made of a glue material which, compared with steel and glass, is so soft that the strain and stress fields in the glue layer are essentially due to the relative horizontal rigid displacement δ of the ring and the plate. In other words, the infinitesimal deformations of the ring and the plate have negligible effects on the strain and the stress fields inside the intermediate zone (for more details, see To et al., 2007).

We consider a horizontal rigid displacement δ of the ring (Fig. 4):

$$\begin{aligned} &u_r(R_3, \theta) = u_\theta(R_3, \theta) = 0, \quad \theta \in [-\pi, \pi], \\ &u_r(R_2, \theta) = \delta \cos\theta, \quad u_\theta(R_2, \theta) = -\delta \sin\theta, \quad \theta \in [-\pi, \pi]. \end{aligned} \tag{3}$$

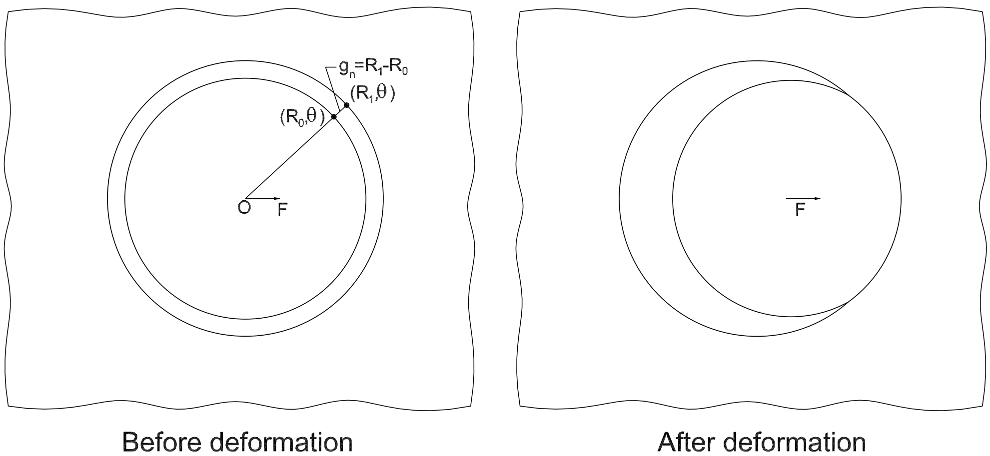

Fig. 2. Bolt in contact with the hole border.

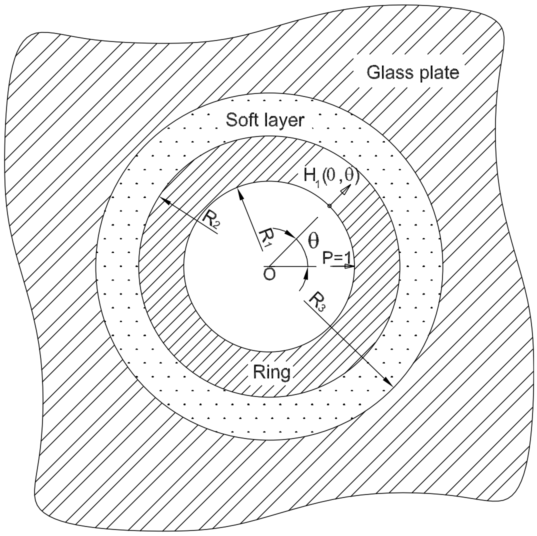

Fig. 3. Ring submitted to a unitary horizontal force.

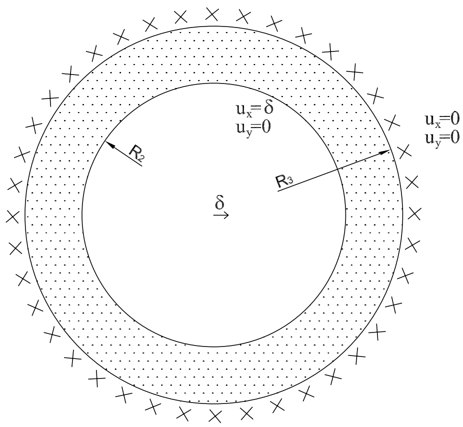

Fig. 4. Simplified model to calculate the stress field in the intermediate layer.

To find the strain and stress fields in the intermediate soft layer, we use the following stress function of Michell's type (see Barber, 2002):

$$\phi_2 = C_1 r^3 \cos\theta + C_2 r\theta \sin\theta + C_3 r \ln r \cos\theta + C_4 r^{-1} \cos\theta. \tag{4}$$

To this stress function (4) are associated the stress field

$$\begin{aligned}
\sigma_{rr}(r,\theta) &= (2C_1 r + 2C_2/r + C_3/r - 2C_4/r^3)\cos\theta,\\
\sigma_{r\theta}(r,\theta) &= (2C_1 r + C_3/r - 2C_4/r^3)\sin\theta,\\
\sigma_{\theta\theta}(r,\theta) &= (6C_1 r + C_3/r + 2C_4/r^3)\cos\theta,
\end{aligned} \tag{5}$$

and the displacement field (see, e.g., Barber, 2002)

$$
\begin{aligned}
u_r(r,\theta) =& \frac{\cos\theta}{2\mu_2}\left[C_1(\kappa_2-2)r^2+\frac{1}{2}((\kappa_2+1)\ln r-1)C_2+\frac{1}{2}((\kappa_2-1)\ln r-1)C_3+C_4r^{-2}\right]\\
&+\frac{\theta\sin\theta}{2\mu_2}[C_2(\kappa_2-1)+C_3(\kappa_2+1)]+\frac{C_5}{2\mu_2}\cos\theta,\\
u_\theta(r,\theta) =& \frac{\sin\theta}{2\mu_2}\left[C_1(\kappa_2+2)r^2-\frac{1}{2}((\kappa_2+1)\ln r+1)C_2-\frac{1}{2}((\kappa_2-1)\ln r+1)C_3+C_4r^{-2}\right]\\
&+\frac{\theta\cos\theta}{2\mu_2}[C_2(\kappa_2-1)+C_3(\kappa_2+1)]-\frac{C_5}{2\mu_2}\sin\theta,
\end{aligned}
\tag{6}
$$

in the bounded region $R_2 \leqslant r \leqslant R_3$. The term $C_5/(2\mu_2)$ in (6) represents a horizontal rigid displacement due to the use of a stress function. The requirement that u_r and u_θ be periodical with respect to θ (Barber, 2002), i.e.,

$$
u_r(r,\theta)=u_r(r,\theta+2\pi),\quad u_\theta(r,\theta)=u_\theta(r,\theta+2\pi) \tag{7}
$$

implies that the terms θ cosθ and θ sinθ in (6) must vanish

$$
C_2(\kappa_2-1)+C_3(\kappa_2+1)=0. \tag{8}
$$

Using the boundary conditions (3) in (6) while accounting for (8), we obtain a system of linear equations for determining the coefficients C_i $(i = 1,2,\ldots,5)$

$$
\begin{cases}
C_1(\kappa_2-2)R_2^2+\frac{C_2}{2}[(\kappa_2+1)\ln R_2-1]+\frac{C_3}{2}[(\kappa_2-1)\ln R_2-1]+C_4R_2^{-2}+C_5=2\delta\mu_2,\\
C_1(\kappa_2+2)R_2^2-\frac{C_2}{2}[(\kappa_2+1)\ln R_2+1]-\frac{C_3}{2}[(\kappa_2-1)\ln R_2+1]+C_4R_2^{-2}-C_5=-2\delta\mu_2,\\
C_1(\kappa_2-2)R_3^2+\frac{C_2}{2}[(\kappa_2+1)\ln R_3-1]+\frac{C_3}{2}[(\kappa_2-1)\ln R_3-1]+C_4R_3^{-2}+C_5=0,\\
C_1(\kappa_2+2)R_3^2-\frac{C_2}{2}[(\kappa_2+1)\ln R_3+1]-\frac{C_3}{2}[(\kappa_2-1)\ln R_3+1]+C_4R_3^{-2}-C_5=0,\\
C_2(\kappa_2-1)+C_3(\kappa_2+1)=0.
\end{cases}
\tag{9}
$$

With the notation $\rho_1=(R_3/R_2)^2$, the solution for the system (9) is given by

$$
\begin{aligned}
C_1 &= \frac{2\delta\mu_2}{R_2^2(2\rho_1-\kappa_2^2\rho_1\ln\rho_1-2-\kappa_2^2\ln\rho_1)},\\
C_2 &= \frac{2(\kappa_2+1)(1+\rho_1)\kappa_2\delta\mu_2}{2\rho_1-\kappa_2^2\rho_1\ln\rho_1-2-\kappa_2^2\ln\rho_1},\\
C_3 &= -\frac{2(\kappa_2-1)(1+\rho_1)\kappa_2\delta\mu_2}{2\rho_1-\kappa_2^2\rho_1\ln\rho_1-2-\kappa_2^2\ln\rho_1},\\
C_4 &= \frac{2R_2^2\rho_1\kappa_2\delta\mu_2}{2\rho_1-\kappa_2^2\rho_1\ln\rho_1-2-\kappa_2^2\ln\rho_1},\\
C_5 &= \frac{4\delta\mu_2(\kappa_2(\rho_1+1)\ln R_3-\rho_1)}{2\rho_1-\kappa_2^2\rho_1\ln\rho_1-2-\kappa_2^2\ln\rho_1}.
\end{aligned}
\tag{10}
$$

By $(5)_1$ and $(5)_2$, the fact that the resultant force applied on the ring is horizontal and unitary gives rise to

$$
r\int_{-\pi}^{\pi}(\sigma_{rr}\cos\theta-\sigma_{r\theta}\sin\theta)\mathrm{d}\theta=-1,
$$

which gives

$$
C_2=-\frac{1}{2\pi}. \tag{11}
$$

Introducing (11) into the expression of C_2 in $(10)_2$, the value of δ is obtained as

$$
\delta=\frac{\kappa_2^2\rho_1\ln\rho_1+2+\kappa_2^2\ln\rho_1-2\rho_1}{4\pi(\kappa_2+1)(1+\rho_1)\kappa_2\mu_2}. \tag{12}
$$

The stress field (5) becomes now explicit as all the coefficients C_i and δ have been specified. The components $\sigma_{rr}(r,\theta)$ and $\sigma_{r\theta}(r,\theta)$ can be written shortly as

$$\sigma_{rr}(r,\,\theta) = \frac{s(r)\cos\theta}{\pi r}, \quad \sigma_{r\theta}(r,\,\theta) = \frac{[s(r)+1]\sin\theta}{\pi r}, \tag{13}$$

where

$$s(r) = \frac{1}{\pi}(2C_1r^2 + 2C_2 + C_3 - 2C_4/r^4).$$

The values of the functions in (13) at $r = R_2$ serve as stress boundary conditions for the ring, which read

$$\sigma_{rr}(R_2,\,\theta) = \frac{s(R_2)\cos\theta}{\pi R_2}, \quad \sigma_{r\theta}(R_2,\,\theta) = \frac{[s(R_2)+1]\sin\theta}{\pi R_2}. \tag{14}$$

2.3. Derivation of the displacement $u_{r1}(\theta)$ on the ring surface

At $r = R_1$, the ring is subjected to a unitary force. Since the Fourier expansion of a point force does not converge, the unitary point force is first considered as a uniformly distributed force in a very small angular interval $[-\epsilon,\epsilon]$ with the intensity $1/(2R_1\epsilon)$ (see, e.g., Timoshenko and Goodier, 1970, p. 136). This stress boundary condition can be expressed by a Fourier series:

$$\begin{aligned}
&\sigma_{rr}(R_1,\,\theta) = -\frac{1}{\pi R_1}\left(\frac{1}{2} + \sum_{n=1}^{\infty}\cos n\theta\frac{\sin n\epsilon}{n\epsilon}\right) \quad \forall\theta\in[-\pi,\pi],\\
&\sigma_{r\theta}(R_1,\,\theta) = 0 \quad \forall\theta\in[-\pi,\pi].
\end{aligned} \tag{15}$$

The Michell stress function for the ring takes the form (see Barber, 2002)

$$\begin{aligned}
\phi_1 = {}& A_{01}r^2 + A_{03}\ln r + A_{11}r^3\cos\theta + A_{12}r\theta\sin\theta + A_{13}r\ln r\cos\theta + A_{14}\cos\theta/r\\
&+ \sum_{n=2}^{\infty}\left(A_{n1}r^{n+2} + A_{n2}r^{-n+2} + A_{n3}r^n + A_{n4}r^{-n}\right)\cos n\theta.
\end{aligned} \tag{16}$$

The stress components $\sigma_{rr}(r,\theta)$ and $\sigma_{r\theta}(r,\theta)$ in the region $R_1 \leqslant r \leqslant R_2$, associated to the stress function ϕ_1, are

$$\begin{aligned}
\sigma_{rr}(r,\,\theta) = {}& 2A_{01} + A_{03}r^{-2}\\
&+ \left(2A_{11}r + 2A_{12}r^{-1} + A_{13}r^{-1} - 2A_{14}r^{-3}\right)\cos\theta\\
&- \sum_{n=2}^{\infty}[(n+1)(n-2)A_{n1}r^n + (n+2)(n-1)A_{n2}r^{-n}\\
&+ n(n-1)A_{n3}r^{n-2} + n(n+1)A_{n4}r^{-n-2}]\cos n\theta,\\
\sigma_{r\theta}(r,\,\theta) = {}& \left(2A_{11}r + A_{13}r^{-1} - 2A_{14}r^{-3}\right)\sin\theta\\
&+ \sum_{n=2}^{\infty}[n(n+1)A_{n1}r^n - n(n-1)A_{n2}r^{-n}\\
&+ n(n-1)A_{n3}r^{n-2} - n(n+1)A_{n4}r^{-n-2}]\sin n\theta.
\end{aligned} \tag{17}$$

These stress components must satisfy the boundary conditions (14) and (15). Thus, we derive a system of linear equations for each value of n. Precisely, three cases need to be distinguished as follows.

(i) For $n = 0$,

$$\begin{cases} 2A_{01} + A_{03}/R_1^2 = -1/(2\pi R_1),\\ 2A_{01} + A_{03}/R_2^2 = 0. \end{cases} \tag{18}$$

(ii) For $n = 1$,

$$\begin{cases} 2R_1A_{11} + 2A_{12}/R_1 + A_{13}/R_1 - 2A_{14}/R_1^3 = -\sin\epsilon/(\epsilon\pi R_1), \\ 2R_1A_{11} + A_{13}/R_1 - 2A_{14}/R_1^3 = 0, \\ 2R_2A_{11} + 2A_{12}/R_2 + A_{13}/R_2 - 2A_{14}/R_2^3 = s(R_2)/(\pi R_2), \\ (\kappa_1 - 1)A_{12} + (\kappa_1 + 1)A_{13} = 0. \end{cases} \tag{19}$$

(iii) For each $n \geqslant 2$,

$$\begin{cases} -(n+1)(n-2)A_{n1}R_1^n - (n+2)(n-1)A_{n2}R_1^{-n} - n(n-1)A_{n3}R_1^{n-2} - n(n+1)A_{n4}R_1^{-n-2} = -\sin n\epsilon/(n\epsilon\pi R_1), \\ n(n+1)A_{n1}R_1^n - n(n-1)A_{n2}R_1^{-n} + n(n-1)A_{n3}R_1^{n-2} - n(n+1)A_{n4}R_1^{-n-2} = 0, \\ -(n+1)(n-2)A_{n1}R_2^n - (n+2)(n-1)A_{n2}R_2^{-n} - n(n-1)A_{n3}R_2^{n-2} - n(n+1)A_{n4}R_2^{-n-2} = 0, \\ n(n+1)A_{n1}R_2^n - n(n-1)A_{n2}R_2^{-n} + n(n-1)A_{n3}R_2^{n-2} - n(n+1)A_{n4}R_2^{-n-2} = 0. \end{cases} \tag{20}$$

Solving the system of linear Equations (18)–(20) gives all the coefficients A_{ni} so that the stress field in the ring is specified. The displacement field corresponding to the stress field is

$$\begin{aligned} u_{r1}(r,\theta) = & \frac{1}{2\mu_1}\big[A_{01}(\kappa-1)r - A_{03}r^{-1} + \cos\theta((\kappa-2)r^2A_{11} \\ & + \frac{1}{2}((\kappa+1)\ln r - 1)A_{12} + \frac{1}{2}((\kappa-1)\ln r - 1)A_{13} + A_{14}r^2) \\ & + \sum_{n=2}^{\infty}\cos n\theta((\kappa-n-1)A_{n1}r^{n+1} + (\kappa+n-1)A_{n2}r^{-n+1} \\ & - nA_{n3}r^{n-1} + nA_{n4}r^{-n-1})\big], \\ u_{\theta 1}(r,\theta) = & \frac{1}{2\mu_1}\Big[\sin\theta((\kappa+2)r^2A_{11} - \frac{1}{2}((\kappa+1)\ln r + 1)A_{12} \\ & - \frac{1}{2}((\kappa-1)\ln r + 1)A_{13} + A_{14}r^2) + \sum_{n=2}^{\infty}\sin n\theta((\kappa+n+1)A_{n1}r^{n+1} \\ & - (\kappa-n+1)A_{n2}r^{-n+1} + nA_{n3}r^{n-1} + nA_{n4}r^{-n-1})\Big]. \end{aligned} \tag{21}$$

Replacing $r = R_1$ in (21)$_1$ and letting $\epsilon \to 0$ so that $\lim_{\epsilon\to 0}\frac{\sin n\epsilon}{n\epsilon} = 1$ for all $n \geqslant 1$, we obtain the radial displacement field on the border caused by the unitary force:

$$H_1(0,\theta) = \frac{1}{\mu_1}\sum_{n=0}^{\infty}A_n\cos n\theta. \tag{22}$$

With the notation $\rho = (R_2/R_1)^2$, the coefficients A_n in the above equation are determined by

$$\begin{aligned} A_0 = & \frac{2\rho + \kappa_1 - 1}{8\pi(\rho-1)}, \\ A_1 = & \frac{1}{8\pi(\kappa_1+1)(\rho^2-1)}\big((1+\kappa_1 - 4\kappa_1\ln R_1)\rho^2 \\ & + [2s(R_2)(\kappa_1^2-1) + (\kappa_1^2 + 2\kappa_1 - 3)]\rho + \kappa_1(4\ln R_1 + \kappa_1 - 3)\big), \\ A_n = & \frac{1}{4\pi(n^2-1)(\rho^{2n} - n^2\rho^{n+1} + 2(n^2-1)\rho^n - n^2\rho^{n-1} + 1)} \\ & \times [(\kappa_1 + n\kappa_1 + n - 1)\rho^{2n} + 2n^2\rho^{n+1} + 2(n^2-1)(\kappa_1-1)\rho^n - \\ & - 2n^2\kappa_1\rho^{n-1} - (1 + n + n\kappa_1 - \kappa_1)] \quad \text{for } n \geqslant 2. \end{aligned} \tag{23}$$

Remark that the displacement and stress fields inside the ring produced by a unitary point force are determined by using the following classical technique: (i) at the beginning, we replace the unitary point force by a uniformly distributed force in a very small angular interval $[-\epsilon, \epsilon]$ so as to be developed into a convergent Fourier series; (ii) at the end, we let $\epsilon \to 0$ to obtain the physically meaningful displacement and stress fields which are regular everywhere except at $\theta = 0$ where the unitary point force is applied. This can be simply seen by studying the convergence of the series specified by Eq. (22).

By superposition, the total radial displacement field resulting from a distributed pressure $p(\xi)$ in the interval $[-\alpha, \alpha]$ can be calculated by

$$u_{r1}(\theta) = R_1 \int_{-\alpha}^{\alpha} H_1(\xi, \theta) p(\xi) \mathrm{d}\xi + \lambda_1 R_1 \cos\theta, \tag{24}$$

in which $H_1(\xi, \theta)$ is defined by

$$H_1(\xi, \theta) = \frac{1}{\mu_1} \sum_{n=0}^{\infty} A_n \cos n(\theta - \xi), \tag{25}$$

and the term $\lambda_1 R_1$ represents a horizontal rigid displacement to be determined by boundary conditions.

2.4. Derivation of the displacement $u_{r0}(\theta)$ on the pin surface

Consider a bolt submitted to two horizontal unitary forces, respectively applied at its frontier and its center in two opposite horizontal directions (Fig. 5). The unitary force at $(r, \theta) = (R_0, 0)$ can be considered as a uniformly distributed pressure of intensity $1/(2R_1\epsilon)$ in a very small interval $[-\epsilon, \epsilon]$, which is expressed by means of a Fourier series as in Eq. (15):

$$\begin{aligned} \sigma_{rr}(R_0, \theta) &= -\frac{1}{\pi R_0}\left(\frac{1}{2} + \sum_{n=1}^{\infty} \cos n\theta \frac{\sin n\epsilon}{n\epsilon}\right) \quad \forall \theta \in [-\pi, \pi], \\ \sigma_{r\theta}(R_0, \theta) &= 0 \quad \forall \theta \in [-\pi, \pi]. \end{aligned} \tag{26}$$

The Michell stress function for the bolt is chosen as (see Barber, 2002)

$$\phi_0 = B_{01} r^2 + B_{11} r^3 \cos\theta + B_{12} r\theta \sin\theta + B_{13} r \ln r \cos\theta + \sum_{n=2}^{\infty} B_{n1} r^{n+2} \cos n\theta + B_{n3} r^n \cos n\theta. \tag{27}$$

Following the same procedure as in the derivation of $u_{r1}(\theta)$, we finally obtain the radial displacement field satisfying the imposed stress boundary conditions. The expression of this displacement on the border at (R_0, θ) is

$$H_0(0, \theta) = \frac{1}{\mu_0} \sum_{n=0}^{\infty} B_n \cos n\theta. \tag{28}$$

The coefficients B_n are specified by

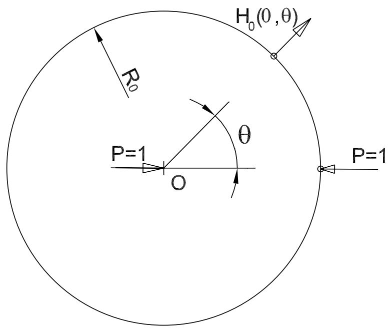

Fig. 5. Pin submitted to a pair of opposite unitary horizontal force.

$$B_0 = -\frac{\kappa_0 - 1}{8\pi},$$
$$B_1 = -\frac{\kappa_0(\kappa_0 - 3 + 4\ln R_1)}{8\pi(\kappa_0 + 1)},$$
$$B_n = -\frac{n\kappa_0 + n + 1 - \kappa_0}{4\pi(n^2 - 1)} \quad \text{for } n \geqslant 2. \tag{29}$$

By superposition, the radial displacement field resulting from a pressure $p(\xi)$ distributed in the interval $[-\alpha, \alpha]$ is

$$u_{r0}(\theta) = R_0 \int_{-\alpha}^{\alpha} H_0(\xi, \theta) p(\xi) \mathrm{d}\xi + \lambda_0 R_0 \cos\theta, \tag{30}$$

with

$$H_0(\xi, \theta) = \frac{1}{\mu_0} \sum_{n=0}^{\infty} B_n \cos n(\theta - \xi). \tag{31}$$

The meaning of $\lambda_0 R_0$ is the same as $\lambda_1 R_1$ in Eq. (24).

2.5. Integral equation for the determination of the contact pressure

Substituting formulae (24) and (30) into the first equation in (2) yields

$$\int_{-\alpha}^{\alpha} [H_0(\xi, \theta) - H_1(\xi, \theta)] p(\xi) \mathrm{d}\xi + (\lambda_0 - \lambda_1)\cos\theta - \frac{\Delta R}{2R}\left[\int_{-\alpha}^{\alpha} [H_0(\xi, \theta) + H_1(\xi, \theta)] p(\xi) \mathrm{d}\xi + (\lambda_0 + \lambda_1)\cos\theta\right] = \frac{\Delta R}{R}, \tag{32}$$

where $R = (R_1 + R_2)/2$. Recall the assumption that ΔR is very small compared with R_1 or R_0, and observe that

$$\frac{1}{2}\left[\int_{-\alpha}^{\alpha} [H_0(\xi, \theta) + H_1(\xi, \theta)] p(\xi) \mathrm{d}\xi + (\lambda_0 + \lambda_1)\cos\theta\right] = \frac{1}{2}\left[\frac{u_{r0}}{R_0} + \frac{u_{r1}}{R_1}\right]$$

is of the same order as $\Delta R/R$. So the third term in the left side of Eq. (32) is of higher order and can be neglected. This implies that Eq. (32) can be simplified into

$$\int_{-\alpha}^{\alpha} [H_0(\xi, \theta) - H_1(\xi, \theta)] p(\xi) \mathrm{d}\xi + (\lambda_0 - \lambda_1)\cos\theta = \frac{\Delta R}{R}. \tag{33}$$

Introducing the expressions (31) and (25) of $H_0(\xi,\theta)$ and $H_1(\xi,\theta)$ into (33) results in

$$\int_{-\alpha}^{\alpha} p(\xi) \sum_{n=0}^{\infty} \left(\frac{A_n}{\mu_1} - \frac{B_n}{\mu_0}\right) \cos n(\theta - \xi) \mathrm{d}\xi + (\lambda_1 - \lambda_0)\cos\theta + \frac{\Delta R}{R} = 0. \tag{34}$$

As $p(\theta)$ is a symmetric function such that $p(\theta) = p(-\theta)$, Eq. (34) can be further reduced to

$$\int_{0}^{\alpha} p(\xi) \sum_{n=0}^{\infty} \left(\frac{A_n}{\mu_1} - \frac{B_n}{\mu_0}\right) \cos n\theta \cos n\xi \mathrm{d}\xi + \frac{\lambda_1 - \lambda_0}{2}\cos\theta + \frac{\Delta R}{2R} = 0. \tag{35}$$

For later use, it is convenient to split this equation as follows

$$\int_0^\alpha p(\xi)\sum_{n=2}^{\infty}\left(\frac{A_n}{\mu_1}-\frac{B_n}{\mu_0}-\frac{n\kappa_1+\kappa_1+n-1}{4\pi(n^2-1)\mu_1}-\frac{n\kappa_0-\kappa_0+n+1}{4\pi(n^2-1)\mu_0}\right)\cos n\theta\cos n\xi \mathrm{d}\xi$$
$$+\int_0^\alpha p(\xi)\sum_{n=2}^{\infty}\left(\frac{n\kappa_1+\kappa_1+n-1}{4\pi(n^2-1)\mu_1}+\frac{n\kappa_0-\kappa_0+n+1}{4\pi(n^2-1)\mu_0}\right)\cos n\theta\cos n\xi \mathrm{d}\xi$$
$$+\sum_{n=0}^{1}\left(\frac{A_n}{\mu_1}-\frac{B_n}{\mu_0}\right)\cos n\theta\int_0^\alpha p(\xi)\cos n\xi \mathrm{d}\xi+\frac{1}{2}(\lambda_1-\lambda_0)\cos\theta+\frac{\Delta R}{2R}=0. \tag{36}$$

Using the value of B_n from (29)$_3$ for $n \geqslant 2$, we obtain

$$\int_0^\alpha p(\xi)\sum_{n=2}^{\infty}\frac{1}{n^2-1}\left(\frac{4\pi(n^2-1)A_n-n(\kappa_1+1)}{4\pi\mu_1}-\frac{\kappa_0-1}{4\pi\mu_0}\right)\cos n\theta\cos n\xi \mathrm{d}\xi$$
$$+\left(\frac{\kappa_1+1}{4\pi\mu_1}+\frac{\kappa_0+1}{4\pi\mu_0}\right)\int_0^\alpha p(\xi)\sum_{n=2}^{\infty}\frac{n}{n^2-1}\cos n\theta\cos n\xi \mathrm{d}\xi$$
$$+\sum_{n=0}^{1}\left(\frac{A_n}{\mu_1}-\frac{B_n}{\mu_0}\right)\cos n\theta\int_0^\alpha p(\xi)\cos n\xi \mathrm{d}\xi+\frac{\lambda_1-\lambda_0}{2}\cos\theta+\frac{\Delta R}{2R}=0. \tag{37}$$

This equation can be rewritten in the compact form

$$\sum_{n=0}^{\infty}K_n\cos n\theta\int_0^\alpha p(\xi)\cos n\xi \mathrm{d}\xi+\int_0^\alpha p(\xi)K(\theta,\xi)\mathrm{d}\xi+\frac{2\pi(\lambda_1-\lambda_0)}{\left(\frac{\kappa_1+1}{\mu_1}+\frac{\kappa_0+1}{\mu_0}\right)}\cos\theta+K$$
$$+\left(\frac{\frac{\kappa_1-1}{\mu_1}-\frac{\kappa_0-1}{\mu_0}}{\frac{\kappa_1+1}{\mu_1}+\frac{\kappa_0+1}{\mu_0}}\right)\sum_{n=2}^{\infty}\frac{\cos n\theta}{n^2-1}\int_0^\alpha p(\xi)\cos n\xi d\xi=0. \tag{38}$$

The function $K(\theta,\xi)$ and the coefficients K_n, K are defined by

$$K(\theta,\xi)=\sum_{n=2}^{\infty}\frac{n}{n^2-1}\cos n\theta\cos n\xi,\quad K=\frac{2\pi\Delta R}{R\left(\frac{\kappa_1+1}{\mu_1}+\frac{\kappa_0+1}{\mu_0}\right)},$$
$$K_n=\frac{4\pi}{\left(\frac{\kappa_1+1}{\mu_1}+\frac{\kappa_0+1}{\mu_0}\right)}\left(\frac{A_n}{\mu_1}-\frac{B_n}{\mu_0}\right)\quad \text{for } n=0 \text{ and } 1,$$
$$K_n=\frac{1}{(n^2-1)\left(\frac{\kappa_1+1}{\mu_1}+\frac{\kappa_0+1}{\mu_0}\right)}\left(\frac{4\pi(n^2-1)A_n-n(\kappa_1+1)}{\mu_1}-\frac{\kappa_1-1}{\mu_1}\right)\quad \text{for } n\geqslant 2. \tag{39}$$

Remark that the function $K(\theta,\xi)$ has the following property

$$\int_0^\theta K(t,\xi)\mathrm{d}t+\frac{\partial K(\theta,\xi)}{\partial\theta}=\sin\theta\cos\xi-\frac{1}{2}\frac{\sin\theta}{\cos\xi-\cos\theta}. \tag{40}$$

Applying the operator $\int_0^\theta(.)\mathrm{d}t+\frac{\partial(.)}{\partial\theta}$ to Eq. (38) and accounting for (40), we obtain

$$\int_0^\alpha p(\xi)\left(\sin\theta\cos\xi-\frac{1}{2}\frac{\sin\theta}{\cos\xi-\cos\theta}\right)\mathrm{d}\xi-\sum_{n=2}^{\infty}\frac{K_n(n^2-1)}{n}\sin n\theta\int_0^\alpha p(\xi)\cos n\xi \mathrm{d}\xi$$
$$+\theta\left(K_0\int_0^\alpha p(\xi)\mathrm{d}\xi+K\right)-\left(\frac{\frac{\kappa_1-1}{\mu_1}-\frac{\kappa_0-1}{\mu_0}}{\frac{\kappa_1+1}{\mu_1}+\frac{\kappa_0+1}{\mu_0}}\right)\sum_{n=2}^{\infty}\frac{\sin n\theta}{n}\int_0^\alpha p(\xi)\cos n\xi d\xi=0. \tag{41}$$

It is seen that by the transformation above, the terms associated to $\cos\theta$ in (34) have disappeared. Noting that

$$\sum_{n=2}^{\infty}\frac{\sin n\theta}{n}\int_0^\alpha p(\xi)\cos n\xi \mathrm{d}\xi=\frac{\pi}{2}\int_0^\theta p(\xi)\mathrm{d}\xi-\frac{\theta}{2}\int_0^\alpha p(\xi)\mathrm{d}\xi-\sin\theta\int_0^\alpha p(\xi)\cos\xi \mathrm{d}\xi, \tag{42}$$

the integral equation (41) for the contact pressure $p(\xi)$ can be recast as

$$\int_0^\alpha \frac{p(\xi)\mathrm{d}\xi}{\cos\theta-\cos\xi} = (\beta_0 G_0+\beta-\gamma G_0)\frac{\theta}{\sin\theta}+(\beta_1-2\gamma)G_1+\sum_{n=2}^{\infty}\beta_n G_n\frac{\sin n\theta}{\sin\theta}+\frac{\gamma\pi}{\sin\theta}\int_0^\theta p(\xi)\mathrm{d}\xi, \tag{43}$$

in which the coefficients β, β_n, and G_n are defined by

$$G_n=\int_0^\alpha p(\xi)\cos n\xi\mathrm{d}\xi,\quad \beta=-2K,\quad \beta_0=-2K_0,\quad \beta_1=-2,$$
$$\beta_n=\frac{2K_n(n^2-1)}{n}\quad \text{for } n\geqslant 2,\quad \gamma=\frac{\frac{\kappa_1-1}{\mu_1}-\frac{\kappa_0-1}{\mu_0}}{\frac{\kappa_1+1}{\mu_1}+\frac{\kappa_0+1}{\mu_0}}. \tag{44}$$

Eq. (43) can be viewed as an extension of the equation [32] in the work of Noble and Hussain (1969) in which the right-hand side contains only the terms $\beta_1 G_1$ and $\beta_0 G_0\theta/\sin\theta$.

In fact, in the work of Noble and Hussain (1969), ΔR was taken to be zero so that $\beta=0$, the plate inside which the hole is located was taken to be infinite so that the right-hand side of Eq. (42) does not occur, and $\gamma=0$. To the best of the authors' knowledge, the integral equation (43) for a finite plate is new.

3. Solutions for the contact pressure and angle in the case $\gamma = 0$

Now, we consider the case where $\gamma=0$, i.e., the second Dundurs coefficient as defined by (44) is equal to zero. This case is important, because the condition $\gamma=0$, or equivalently $(\kappa_1-1)/\mu_1=(\kappa_2-1)/\mu_2$, is satisfied in a number of situations of practical interest. For example, this condition is trivially met when the pin and the ring are made of the same material. Assuming $\gamma=0$, Eq. (43) is simplified and becomes

$$\int_0^\alpha \frac{p(\xi)\mathrm{d}\xi}{\cos\theta-\cos\xi} = (\beta_0 G_0+\beta)\frac{\theta}{\sin\theta}+\beta_1 G_1+\sum_{n=2}^{\infty}\beta_n G_n\frac{\sin n\theta}{\sin\theta}. \tag{45}$$

As shown above, the third term in the right-hand side of Eq. (45) allows to account for the finiteness of the reinforcement ring (Fig. 1). Combining the definition $(44)_5$ of $\beta_n (n\geqslant 2)$ and the two expressions $(39)_4$ and $(23)_3$ of K_n and A_n, we can specified β_n as

$$\beta_n=\frac{2}{1+\frac{\kappa_0+1}{\kappa_1+1}\frac{\mu_1}{\mu_0}}\frac{(n^2+n)\rho^{n+1}-2(n^2-1)\rho^n+(n^2-n)\rho^{n-1}-2}{\rho^{2n}-n^2\rho^{n+1}+2(n^2-1)\rho^n-n^2\rho^{n-1}+1}\quad \text{for } n\geqslant 2. \tag{46}$$

It is important to remark that the expression (46) of β_n $(n\geqslant 2)$ has the property that β_n tends to 0 as $n\to\infty$ with exponential rate ρ^{-n+1}. Thus for each prescribed value of ρ, the infinite series $\sum_{n=2}^{\infty}\beta_n\frac{\sin n\theta\cos n\xi}{\sin\theta}$ can approximated with a prescribed precision by a finite series $\sum_{n=2}^{k}\beta_n\frac{\sin n\theta\cos n\xi}{\sin\theta}$. In this way, the governing integral equation (45) is reduced to

$$\int_0^\alpha \frac{p(\xi)\mathrm{d}\xi}{\cos\theta-\cos\xi} = (\beta_0 G_0+\beta)\frac{\theta}{\sin\theta}+\beta_1 G_1+\sum_{n=2}^{k}\beta_n G_n\frac{\sin n\theta}{\sin\theta}. \tag{47}$$

3.1. General solution for the contact pressure

Eq. (47) can be transformed into a singular integral equation (Cauchy kernel type) by the change of variables

$$x=\sin^2(\theta/2)/m,\quad t=\sin^2(\xi/2)/m,\quad m=\sin^2(\alpha/2). \tag{48}$$

This implies

$$\theta=\arccos(1-2xm),\quad \xi=\arccos(1-2tm). \tag{49}$$

With the help of (48), Eq. (47) takes the form

$$\int_0^1 \frac{p_1(t)\mathrm{d}t}{t-x} = F(x), \quad 0 \leqslant x \leqslant 1, \tag{50}$$

with

$$p_1(t(\xi)) = \frac{p(\xi)}{\sin\xi}, \quad F(x(\theta)) = (\beta_0 G_0 + \beta)\frac{\theta}{\sin\theta} + \sum_{n=1}^{k} \beta_n G_n \frac{\sin n\theta}{\sin\theta}. \tag{51}$$

The expression for $p(\xi)$ is obtained by solving the Cauchy singular integral equation (50) as in Peters (1963) and using $(51)_1$:

$$p(\xi) = \frac{C\sin\xi}{\pi\sqrt{t(1-t)}} - \frac{\sin\xi}{\pi^2\sqrt{t}}\frac{\mathrm{d}}{\mathrm{d}t}\int_t^1 \frac{\mathrm{d}\sigma}{\sqrt{\sigma-t}}\int_0^\sigma \frac{F(x)\sqrt{x}\mathrm{d}x}{\sqrt{\sigma-x}}, \tag{52}$$

in which the constant C is determined by

$$C = \int_0^1 p_1(t)\mathrm{d}t = \frac{1}{2\sin^2\alpha/2}\int_0^\alpha p(\xi)\mathrm{d}\xi = \frac{G_0}{2m}.$$

Accounting for $(48)_2$, the first term of (52) becomes

$$\frac{C\sin\xi}{\pi\sqrt{t(1-t)}} = \frac{\sqrt{2}G_0\cos\xi/2}{\pi\sqrt{\cos\xi-\cos\alpha}} = \frac{G_0\cos\xi/2}{\pi\sqrt{m-\sin^2\xi/2}}. \tag{53}$$

To integrate the second term of (52), we first define $P_n(\xi)$ by

$$\begin{aligned} P_0(\xi) &= \sin\xi\frac{1}{\pi^2\sqrt{t}}\frac{\mathrm{d}}{\mathrm{d}t}\int_t^1 \frac{\mathrm{d}\sigma}{\sqrt{\sigma-t}}\int_0^\sigma \frac{\theta}{\sin\theta}\frac{\sqrt{x}\mathrm{d}x}{\sqrt{\sigma-x}}, \\ P_n(\xi) &= \sin\xi\frac{1}{\pi^2\sqrt{t}}\frac{\mathrm{d}}{\mathrm{d}t}\int_t^1 \frac{\mathrm{d}\sigma}{\sqrt{\sigma-t}}\int_0^\sigma \frac{\sin n\theta}{\sin\theta}\frac{\sqrt{x}\mathrm{d}x}{\sqrt{\sigma-x}} \quad \text{for } n \geqslant 1. \end{aligned} \tag{54}$$

According to Noble and Hussain (1969),

$$P_0(\xi) = \frac{2}{\pi}\left(\frac{\ln(1-m)\cos\xi/2}{2\sqrt{m-\sin^2\xi/2}} + \ln\left|\frac{\cos\xi/2+\sqrt{m-\sin^2\xi/2}}{\sqrt{1-m}}\right|\right). \tag{55}$$

Concerning $P_n(\xi)(n \geqslant 1)$, we invoke the variable change $(49)_1$ and then make the integration to arrive at

$$P_n(\xi) = \cos\xi/2\left(\frac{Q_n(m)}{\sqrt{m-\sin^2\xi/2}} + R_n(\sin^2\xi/2)\sqrt{m-\sin^2\xi/2}\right). \tag{56}$$

Here, for each $n \geqslant 1$, $Q_n(m)$ is a polynomial of m, $R_n(\sin^2\xi/2)$ is a polynomial of $\sin^2\xi/2$ whose coefficients depend on m.

Using superposition, we can deduce

$$p(\xi) = G_0\left(\frac{\cos\xi/2}{\pi\sqrt{m-\sin^2\xi/2}} - \beta_0 P_0(\xi)\right) - \beta P_0(\xi) - \sum_{n=1}^{k}\beta_n G_n P_n(\xi). \tag{57}$$

Due to the definition $(44)_1$, the coefficients G_n are related to each other by a system of k linear equations with $k+1$ variables $G_0, G_1, \ldots, G_k$:

$$G_0 \int_0^{\alpha} \left(\frac{\cos \xi/2}{\pi\sqrt{m - \sin^2 \xi/2}} - \beta_0 P_0(\xi) \right) \cos n\xi \mathrm{d}\xi - \beta \int_0^{\alpha} P_0(\xi) \cos n\xi \mathrm{d}\xi$$
$$- \sum_{i=1}^{k} G_i \int_0^{\alpha} \beta_i P_i(\xi) \cos n\xi \mathrm{d}\xi = G_n \quad \text{for } n = 1, 2, \ldots, k, \tag{58}$$

where use is made of (57). In addition, the force equilibrium requires

$$G_1 = \int_0^{\alpha} p(\xi) \cos \xi \mathrm{d}\xi = F/2R. \tag{59}$$

The system of Eqs. (58) and (59) now allows us to determine all the coefficients and obtain the contact pressure.

To avoid the occurrence of a singular value of $p(\xi)$ for the problem investigated in the present paper (see, e.g., Hills et al., 1992), we must have

$$\frac{G_0}{\pi} - \sum_{n=1}^{k} \beta_n G_n Q_n(m) - \frac{1}{\pi} \ln(1 - m)(\beta_0 G_0 + \beta) = 0. \tag{60}$$

This nonlinear equation in terms of n is derived by introducing (55) and (56) into (57) and requiring that the sum of the terms containing $\frac{1}{\sqrt{m-\sin^2 \xi/2}}$ be zero.

Eliminating the terms relating to $\frac{1}{\sqrt{m-\sin^2 \xi/2}}$, Eqs. (57) and (58) become, respectively

$$p(\xi) = -\frac{2(\beta_0 G_0 + \beta)}{\pi} \ln \left| \frac{\cos \xi/2 + \sqrt{m - \sin^2 \xi/2}}{\sqrt{1 - m}} \right|$$
$$- \sum_{i=1}^{k} \beta_i G_i R_n(\sin^2 \xi/2) \sqrt{m - \sin^2 \xi/2} \cos \xi/2, \tag{61}$$

$$- \frac{2(\beta_0 G_0 + \beta)}{\pi} \int_0^{\alpha} \ln \left| \frac{\cos \xi/2 + \sqrt{m - \sin^2 \xi/2}}{\sqrt{1 - m}} \right| \cos n\xi \mathrm{d}\xi$$
$$- \sum_{i=1}^{k} \beta_i G_i \int_0^{\alpha} R_n(\sin^2 \xi/2) \sqrt{m - \sin^2 \xi/2} \cos \xi/2 \cos n\xi \mathrm{d}\xi$$
$$= G_n \quad \text{for } n = 1, 2, \ldots k. \tag{62}$$

From (59), (61) and (62), several conclusions can be drawn:

Case 1: if $\beta = 0$ (i.e., $\Delta R = 0$), then the coefficients G_i are linearly proportional to total force F while α is independent of F.
Case 2: if $\beta \neq 0$ (i.e., $\Delta R \neq 0$), then $\beta_0 G_0 + \beta$ and G_i ($i \geqslant 1$) are linearly proportional to the total force F but the contact angle 2α depends on the force F by the nonlinear equation (60).

3.2. Application to the case $k = 2$

Taking $k = 2$, the nonlinear equation (60) is considerably simplified as

$$G_0 - (G_0\beta_0 + \beta) \ln(1 - m) + \beta_1 G_1 m - \beta_2 G_2 m(3m - 2) = 0, \tag{63}$$

and Eq. (61) becomes

$$p(\xi) = -\frac{2(\beta_0 G_0 + \beta)}{\pi} \ln\left|\frac{\cos\xi/2 + \sqrt{m - \sin^2\xi/2}}{\sqrt{1-m}}\right| + \frac{8\beta_2 G_2}{\pi}\cos\xi/2\sin^2\xi/2\sqrt{m-\sin^2\xi/2}$$
$$-\frac{2\cos\xi/2}{\pi}\sqrt{m-\sin^2\xi/2}[\beta_1 G_1 + 2(1-m)\beta_2 G_2]. \tag{64}$$

Using the formulae in the appendix for the integrals in (62), the relations between G_n are specified by

$$\begin{cases} -m(\beta_0 G_0 + \beta) - \frac{m(2-m)}{2}\beta_1 G_1 - 2m(1-2m+m^2)\beta_2 G_2 = G_1, \\ -\frac{m(2-3m)}{2}(\beta_0 G_0 + \beta) - m(1-2m+m^2)\beta_1 G_1 - \frac{m(4-14m+20m^2-9m^3)}{2}\beta_2 G_2 = G_2. \end{cases} \tag{65}$$

From these two equations and (59), we can express G_0 and G_2 in terms of F:

$$G_2 = \frac{F(\beta_1 m^3 + 6m - 4)}{4R(3\beta_2 m^4 - 4\beta_2 m^3 - 2)},$$
$$G_0 = \frac{F}{4Rm\beta_0(3\beta_2 m^4 - 4\beta_2 m^3 - 2)}\big(\beta_1\beta_2(m^6 - 6m^5 + 6m^4) - \beta_2(18m^4 - 40m^3 + 28m^2 - 8m)$$
$$-\beta_1(2m^2 - 4m) + 4\big) - \frac{\beta}{\beta_0}. \tag{66}$$

By putting (66) into Eq. (63), we obtain the nonlinear relation between m and the applied force F. Solving this equation gives m and the contact angle 2α by $(48)_3$. Finally the pressure is given by (64).

3.3. Validation by the finite element method (FEM) for $k = 2$

To validate the approximative closed-form solution for $k = 2$ and identify its application domain, we use the finite element method. A square glass plate of dimension $200 \times 200 \times 19$ mm with a pin joint (Fig. 6) is simulated using the program MSC MARC. The following parameters are used:

Geometric parameters: R_0=14.75 mm or 15 mm, $R_1 = 15$ mm, $R_2 = 30$ mm or 45 mm, $R_3 = 60$ mm, $L = 200$ mm (width and length of the glass plate), $e = 19$ mm (thickness of the glass plate);
Bolt ($r \leqslant R_0$): $E_0 = 200$ GPa, $\nu_0 = 0.3$;
Ring ($R_1 \leqslant r \leqslant R_2$): $E_1 = 200$ GPa, $\nu_1 = 0.3$;
Soft layer ($R_2 \leqslant r \leqslant R_3$): $E_2 = 2$ GPa, $\nu_2 = 0.2$;
Glass plate ($R_3 \leqslant r$ and $|x| \leqslant L/2$ and $|y| \leqslant L/2$): $R_3 = 60$ mm, $E_3 = 70$ GPa, $\nu_3 = 0.2$;
Total force $P = P_x = 100$ kN applied at the center of the bolt. Force per thickness is equal $F = P/e = 100/19$ (kN/mm);

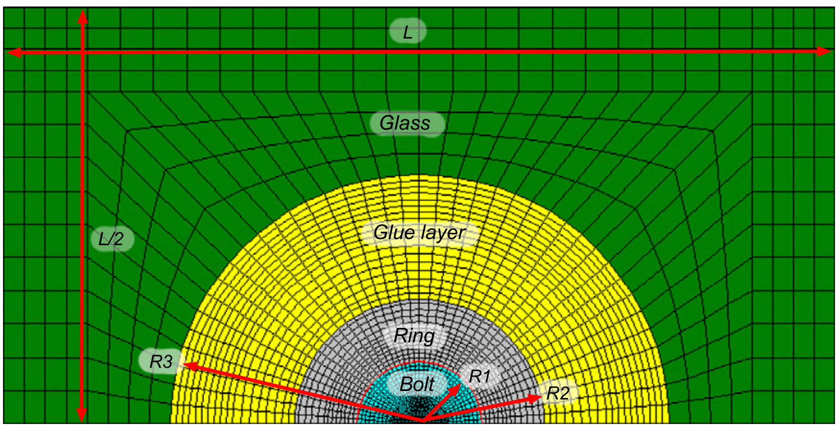

Fig. 6. Mesh of one half of a glass structure.

Boundary conditions: $u_x(x = -L/2, y) = 0$, $u_y(x, y = 0) = 0$.

The glass structure is analyzed by using the plane stress assumption and its symmetry property. Its mesh is shown in Fig. 6.

Case 1. R_0=15 mm ($\Delta R = 0$). The parameters involved and the results obtained by the analytic solution are given as below

R_2	ρ	β	β_0	β_1	β_2	m	α	G_0	G_1	G_2
∞	∞	0.00	−0.5	−2	0	0.455	84.83	231.1	176.9	–
45	9.00	0.00	−0.56	−2	0.95	0.471	86.71	237.8	176.9	54.11
30	4.00	0.00	−0.67	−2	3.63	0.489	88.70	248.6	176.9	37.45

Case 2. $R_0 = 14.75$ mm ($\Delta R = 0.25$ mm). The parameters involved and the results provided by the analytic solution are specified as below

R_2	ρ	β	β_0	β_1	β_2	m	α	G_0	G_1	G_2
45	9.00	2640	−0.56	−2	0.95	0.063	29.02	182.7	176.9	160.2
30	4.00	2640	−0.67	−2	3.63	0.082	33.28	184.8	176.9	154.6

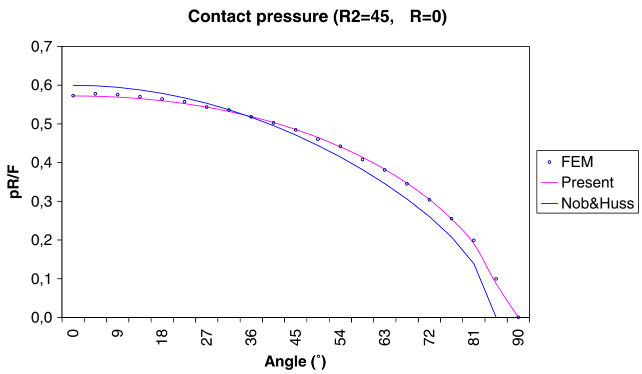

Fig. 7. Contact pressure and angle when $R_2 = 45$, $R_2/R_1 = 3$, $\Delta R = 0$.

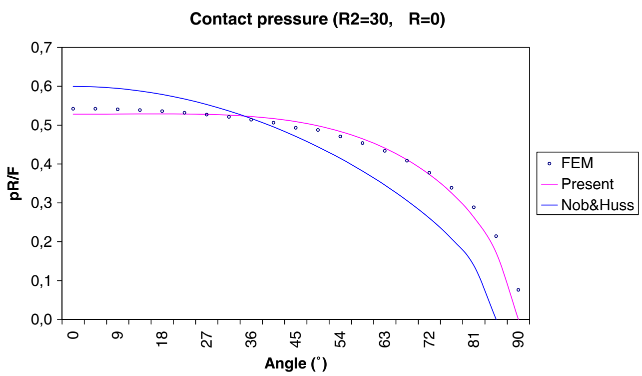

Fig. 8. Contact pressure and angle when $R_2 = 30$, $R_2/R_1 = 2$, $\Delta R = 0$.

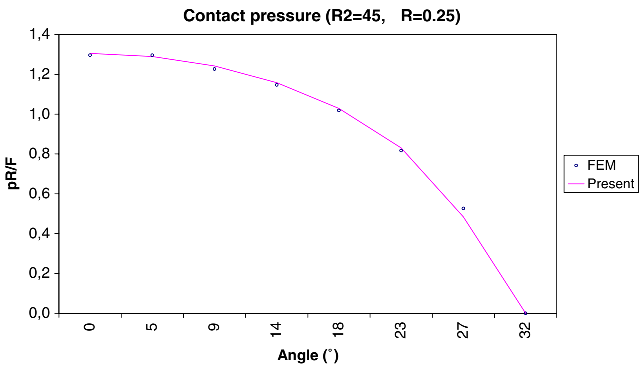

Fig. 9. Contact pressure and angle when $R_2 = 45$, $R_2/R_1 = 3$, $\Delta R = 0.25$.

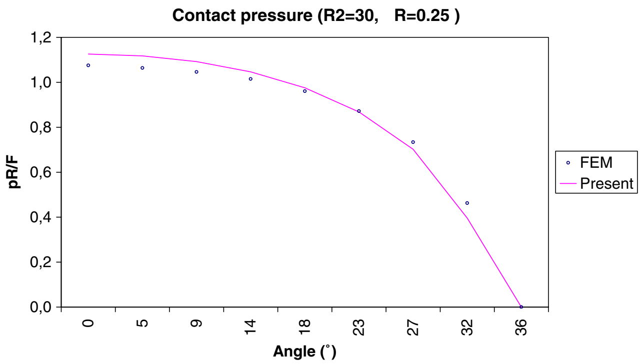

Fig. 10. Contact pressure and angle when $R_2 = 30$, $R_2/R_1 = 2$, $\Delta R = 0.25$.

The contact pressures calculated by the analytic and the numerical solutions are plotted in Figs. 7–10 where the horizontal axis represents angles ξ, and the vertical axis represents the scalar $p(\xi)R/F$. From these graphs, a good agreement is seen to exist between the analytical and numerical results in terms of the contact pressure and angle. At the same time, an important deviation is observed between the FE results and the ones obtained by the formula of Noble and Hussain (1969) derived for the case $R_2/R_1 = \infty$.

4. Final remarks

In this work, a closed-form solution is given for the conforming contact problem of reinforced pin-loaded joints used in glass structures. The fact that the glue layer (Fig. 1) is made of a very soft material makes it possible to analytically determine the strain and stress fields inside the glue layer. To solve the bolt-ring contact problem, the method proposed by Noble and Hussain (1969) has been extended to the case of a finite two-dimensional body. When the ratio $R_2/R_1 \geqslant 2$, the obtained approximate analytical solutions have been shown to be in very good agreement with the numerical results issue from the finite element method. If $R_2/R_1 < 2$, the convergence of the series in (43) becomes slower and a longer finite sum ($k \geqslant 3$) should be used in (47). In this case, the method presented in 3.1 is still valid and efficient but more complicated computations are involved.

In Section 3, the second Dundurs coefficient γ is taken to be zero. This is sufficient for our problem where the bolt and ring in a pin-loaded joint are usually made of the same material, i.e. steel. However, from the theoretical standpoint, it is interesting to know how to obtain an analytical approximate solution for the integral equation (43) when $\gamma \neq 0$. This problem is under investigation.

Taking into account the friction between the bolt and ring is an additional aspect to be treated. A closed-form solution for the resulting frictional contact problem seems very difficult to obtain, and the use of a numerical method, such as the finite element method, appears thus necessary to solving it.

Acknowledgment

The authors address their special thanks to the reviewers for the useful comments.

Appendix A

The following formulae are needed to calculate the integrals in the system of Eq. (65) (with $m = \sin^2\alpha/2$):

$$\int_0^\alpha \ln\left|\frac{\cos\xi/2 + \sqrt{m - \sin^2\xi/2}}{\sqrt{1-m}}\right|\cos\xi \mathrm{d}\xi = \frac{\pi}{2}m,$$

$$\int_0^\alpha \ln\left|\frac{\cos\xi/2 + \sqrt{m - \sin^2\xi/2}}{\sqrt{1-m}}\right|\cos 2\xi \mathrm{d}\xi = \frac{\pi}{4}m(2-3m),$$

$$\int_0^\alpha \cos\xi/2\sqrt{m - \sin^2\xi/2}\cos\xi \mathrm{d}\xi = \frac{\pi}{4}m(2-m),$$

$$\int_0^\alpha \cos\xi/2\sqrt{m - \sin^2\xi/2}\cos 2\xi \mathrm{d}\xi = \frac{\pi}{2}m(1-2m+m^2),$$

$$\int_0^\alpha \cos\xi/2\sqrt{m - \sin^2\xi/2}\sin^2\xi/2\cos\xi \mathrm{d}\xi = \frac{\pi}{8}m^2(1-m),$$

$$\int_0^\alpha \cos\xi/2\sqrt{m - \sin^2\xi/2}\sin^2\xi/2\cos 2\xi \mathrm{d}\xi = \frac{\pi}{16}m^2(2-8m+5m^2).$$

References

Barber, J.R., 2002. Elasticity. Kluwer Academic Publisher, Dordrecht.

Ciavarella, M., Baldini, A., Barber, J.R., Strozzi, A., 2006. Reduced dependence on loading parameters in almost conforming contacts. Int. J. Mechanical Sciences 48, 917–925.

Ciavarella, M., Decuzzi, P., 2001. The state of stress induced by the plane frictionless cylindrical contact. I. The case of elastic similarity. Int. J. Solids Struct. 38, 4525–4533.

Hills, D.A., Nowell, D., Sackfield, A., 1992. Mechanics of Elastic Contacts. Butterworth-Heinemann.

Hyer, M.W., Klang, E.C., 1985. Contact stresses in pin-loaded orthotropic plates. Int. J. Solids Struct. 21, 957–975.

Iyer, K., 2001. Solutions for contact in pinned connections. Int. J. Solids Struct. 38, 9133–9148.

Lin, C.C., Lin, C.H., 1999. Stresses around pin-loaded hole in composite laminates using direct boundary element method. Int. J. Solids Structures 36, 763–783.

Noble, B., Hussain, M.A., 1969. Exact solution of certain dual series for indentation and inclusion problem. Int. J. Eng. Sci. 7, 1149–1161.

Peters, A.S., 1963. A note on the integral equation of the first kind with a Cauchy kernel. Commun. Pure Appl. Math. 16, 57–61.

Rao, A.K., 1978. Elastic analysis of pin joints. Computers and Structures 9, 125–144.

Timoshenko, S., Goodier, J.N., 1970. Theory of Elasticity. Mc Graw-Hill, New York.

To, Q.D., He, Q.-C., Cossavella, M., Morcant, K., Panait, A., 2007. Stress analysis of the intermediate soft layer in a reinforced pin loaded joint used in glass structures, submitted for publication.